

# UC San Diego

## UC San Diego Previously Published Works

### Title

Fat suppression for ultrashort echo time imaging using a novel soft-hard composite radiofrequency pulse.

### Permalink

<https://escholarship.org/uc/item/6f8807v1>

### Journal

Magnetic resonance in medicine, 82(6)

### ISSN

0740-3194

### Authors

Ma, Ya-Jun  
Jerban, Saeed  
Jang, Hyungseok  
[et al.](#)

### Publication Date

2019-12-01

### DOI

10.1002/mrm.27885

Peer reviewed

## NOTE

# Fat suppression for ultrashort echo time imaging using a novel soft-hard composite radiofrequency pulse

Ya-Jun Ma<sup>1</sup>  | Saeed Jerban<sup>1</sup> | Hyungseok Jang<sup>1</sup>  | Eric Y. Chang<sup>1,2</sup> | Jiang Du<sup>1</sup>

<sup>1</sup>Department of Radiology, University of California, San Diego, California

<sup>2</sup>Radiology Service, VA San Diego Healthcare System, San Diego, California

## Correspondence

Jiang Du, Department of Radiology,  
University of California, San Diego,  
200 West Arbor Drive, San Diego,  
CA 92103-8226.

Email: jiangdu@ucsd.edu

## Funding information

GE Healthcare, NIH, Grant/Award  
Numbers: 1R01 AR062581, 1R01  
AR068987 and 1R21 AR073496; VA  
Clinical Science R&D Service, Grant/  
Award Numbers: I01CX001388 and  
I01RX002604

**Purpose:** To design a soft-hard composite pulse for fat suppression and water excitation in ultrashort echo time (UTE) imaging with minimal short  $T_2$  signal attenuation.

**Methods:** The composite pulse contains a narrow bandwidth soft pulse centered on the fat peak with a small negative flip angle ( $-\alpha$ ) and a short rectangular pulse with a small positive flip angle ( $\alpha$ ). The fat magnetization experiences both tipping-down and -back with an identical flip angle and thus returns to the equilibrium state, leaving only the excited water magnetization. Bloch simulations, as well as knee, tibia, and ankle UTE imaging studies, were performed to investigate the effectiveness of fat suppression and corresponding water signal attenuation. A conventional fat saturation (FatSat) module was used for comparison. Signal suppression ratio (SSR), defined as the ratio of signal difference between non-fat-suppression and fat-suppression images over the non-fat-suppression signal, was introduced to evaluate the efficiency of the composite pulse.

**Results:** Numerical simulations demonstrate that the soft-hard pulse has little saturation effect on short  $T_2$  water signals. Knee, tibia, and ankle UTE imaging results suggest that comparable fat suppression can be achieved with the soft-hard pulse and the FatSat module. However, much less water saturation is induced by the soft-hard pulse, especially for short  $T_2$  tissues, with SSRs reduced from  $71.8 \pm 6.9\%$  to  $5.8 \pm 4.4\%$  for meniscus, from  $68.7 \pm 5.5\%$  to  $7.7 \pm 7.6\%$  for bone, and from  $62.9 \pm 12.0\%$  to  $4.8 \pm 3.2\%$  for the Achilles tendon.

**Conclusion:** The soft-hard composite pulse can suppress fat signals in UTE imaging with little signal attenuation on short  $T_2$  tissues.

## KEYWORDS

fat suppression, soft-hard composite pulse, ultrashort echo time

## 1 | INTRODUCTION

Ultrashort echo time (UTE) sequences with echo times  $<100 \mu\text{s}$  can detect fast decaying signals and provide a much higher signal to noise ratio for short  $T_2$  tissues than conventional clinical gradient recalled echo-type sequences with much

longer echo times.<sup>1</sup> In the past decade, these UTE sequences have been widely investigated for both morphological and quantitative imaging of short  $T_2$  tissues, including calcified cartilage, menisci, tendons, ligaments, bone, and myelin.<sup>2-7</sup>

Fat suppression is very important for UTE imaging of musculoskeletal tissues.<sup>8-10</sup> This is because UTE imaging

tends to show a high fat signal, attributed to fat's high proton density and short  $T_1$  value, which lead to low contrast for short  $T_2$  tissues. Additionally, UTE imaging of short  $T_2$  tissues often suffers from fat contamination attributed to partial volume effect, as well as from off-resonance artifacts induced by non-Cartesian UTE acquisition. Thus, for both high contrast morphological imaging and accurate quantitative imaging of short  $T_2$  tissues, it is crucial to incorporate fat-suppression techniques with UTE imaging.

The most commonly used approach for fat suppression in clinical practice is the chemical shift-based fat saturation (also called FatSat module), which includes a spectrally selective radiofrequency (RF) pulse followed by a gradient spoiler. However, the FatSat module is not well suited for short  $T_2$  imaging because of its strong direct attenuation of the broad frequency spectrum of short  $T_2$  tissues.<sup>11</sup> Furthermore, a relatively large saturation flip angle (i.e., no less than  $90^\circ$ ) is used in the FatSat module, which also leads to indirect signal attenuation induced by the magnetization transfer (MT) effects, especially for the collagen-rich tissues.<sup>12</sup> Other techniques, such as the long  $T_2$  suppression RF pulse<sup>13,14</sup> or the inversion recovery preparations,<sup>15-18</sup> can generate high contrast in morphological UTE imaging of short  $T_2$  tissues. However, they can only be conditionally useful for quantitative UTE imaging because the long  $T_1$  components in short  $T_2$  tissues are also partially suppressed by these techniques.<sup>19,20</sup> Moreover, fat-separation-based methods, such as the single-point Dixon, iterative decomposition of water and fat with echo asymmetry and least-squares estimation and UTE spectroscopic imaging, can be incorporated in both morphological and quantitative UTE imaging.<sup>21-23</sup> However, they require longer acquisition time and data postprocessing.

In this study, we proposed a new fat-suppression RF pulse for UTE imaging of short  $T_2$  tissues with well-preserved short  $T_2$  signals using a soft-hard composite pulse. Bloch simulations were performed to investigate its signal attenuation effects on both short and long  $T_2$  tissues, which were then compared with both nonfat suppression excitation and the conventional FatSat technique. Then, in vivo knee and tibia as well as ex vivo ankle UTE imaging studies were performed to evaluate the effectiveness of fat suppression and investigate the corresponding short  $T_2$  signal attenuation for both the proposed soft-hard composite pulse and the conventional FatSat module.

## 2 | METHODS

### 2.1 | Soft-hard composite pulse design

Features of the newly designed soft-hard composite pulse and the conventional FatSat module are both shown in Figure 1. The proposed fat-suppression pulse or water-excitation pulse consists of 2 RF pulses: 1 soft pulse (minimum-phase

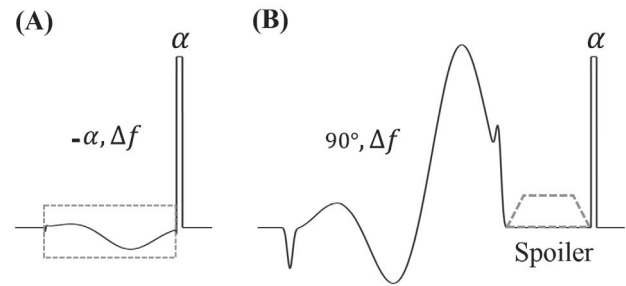


**FIGURE 1** The proposed soft-hard composite pulse (A) and the conventional FatSat module (B). A soft RF pulse centered on fat on-resonance frequency ( $\Delta f$ ) with a negative flip angle ( $-\alpha$ ) was used to flip the fat magnetization only, followed by a short hard pulse with a positive flip angle ( $\alpha$ ) to flip all the magnetizations in the opposite direction (A). The commonly used FatSat module is shown in (B) for comparison. A  $90^\circ$  soft pulse centered on fat on-resonance frequency was used to flip down the fat magnetization, and then all the excited transverse magnetizations were crushed by a gradient spoiler. A following hard pulse was used for water signal excitation. The RF phases of soft pulses in (A) and (B) were determined by their center frequencies

Shinnar–Le Roux [mip-SLR] design with a duration of 4.4 ms and spectral bandwidth of 500 Hz) and 1 hard pulse (Figure 1A).<sup>24</sup> The soft pulse centers on the fat peak with a narrow bandwidth. It is used to flip only the fat magnetization and is followed by a short hard pulse with the same flip angle as the soft pulse, which flips both water and fat magnetizations in the opposite direction. Given that the fat magnetization experiences both tipping down and tipping back with this identical flip angle, most of the fat magnetization returns to the equilibrium state. Subsequently, most of the fat signals are not received by the subsequent UTE acquisitions. In addition, the soft pulse has been designed with a narrow bandwidth and with a pulse duration of several milliseconds; thus, the RF power of the soft pulse is relatively low. The soft pulse excitation is therefore expected to have little saturation effect on the water magnetizations. This makes it possible for the water signals to be effectively excited by the following hard pulse.

The conventional FatSat technique consists of a saturation pulse (mip-SLR design with a duration of 8 ms and bandwidth of 500 Hz) centered on the fat peak with a flip angle no less than  $90^\circ$ , followed by a gradient spoiler to crush all the excited transverse magnetizations (Figure 1B). Then, a short hard pulse is utilized for signal excitation.

Typically, the flip angle of the soft pulse (the same as the excitation flip angle) in the soft-hard composite pulse is much lower than  $90^\circ$  for UTE imaging. Therefore, both direct and indirect saturations (i.e., MT effect) of the water signals produced by the soft pulse in the proposed soft-hard composite pulse are much less than the water-signal attenuations induced by the FatSat module.

## 2.2 | Numerical simulations

Bloch simulation was carried out to compare the excitations of a single hard pulse, the proposed soft-hard composite pulse, and the conventional FatSat module for both short and long  $T_2$  imaging with tissue  $T_2$ s of 0.3, 0.5, 1, 2, 5, and 20 ms. The  $T_2$  of fat was 20 ms. The excitation flip angle was set to  $10^\circ$  for all 3 RF pulses in simulation; the other parameters were as follows: (1) the single hard pulse: duration was 50  $\mu$ s; (2) the soft-hard composite pulse: mip-SLR design, 4.4 ms, bandwidth of 500 Hz, and center frequency of  $-440$  Hz (i.e., off-resonance frequency of fat at 3T); hard pulse duration was 50  $\mu$ s; (3) the GE product FatSat module: mip-SLR design, 8 ms, bandwidth of 500 Hz, center frequency of  $-440$  Hz, and flip angle of  $90^\circ$ ; the spoiler gradient area was large enough to keep the dephasing in a single voxel no less than  $4\pi$ ; the duration of hard pulse excitation was 50  $\mu$ s.

Numerical simulations for UTE acquisitions were also performed to compare the signal intensities using excitations of the single hard pulse, the proposed soft-hard composite pulse, and the FatSat module. Identical pulse shapes, as above, were utilized in this simulation; other sequence parameters were as follows: TR = 50 ms, nominal TE = 20  $\mu$ s, and excitation flip angles ranged from  $0^\circ$  to  $50^\circ$ . A constant  $T_1$  value of 800 ms and variable  $T_2$  values of 0.3, 0.5, 1, 2, 5, and 20 ms were used for simulation. The nominal TE is defined as the time between the end of the hard pulse and the k-space center.

## 2.3 | UTE imaging

To compare UTE imaging with and without fat suppression, in vivo knee and tibia imaging, as well as ex vivo ankle imaging, was performed on a 3T whole-body scanner (GE Healthcare Technologies, Milwaukee, WI). An 8-channel transmit/receive knee coil was used for both RF transmission and signal reception. A 3D UTE-Cones sequence was used for both short and long  $T_2$  tissue imaging with unique k-space trajectories that sampled data along evenly spaced twisting paths in the shape of multiple cones.<sup>17,18</sup> Data sampling started at the center of k-space as soon as possible after the RF excitation with a minimal nominal TE of 32  $\mu$ s.

Fat suppression was carried out using both the proposed soft-hard composite pulse and the GE product FatSat module. The single hard pulse excitation UTE imaging without fat suppression was also utilized for comparison. All the RF pulse shapes are identical to the pulses used in the simulation section. The following UTE imaging sequences were repeated using the above 3 excitation pulses, respectively. Five healthy volunteers (22–35 years old) were recruited for knee joint imaging; the sequence parameters of 3D UTE-Cones were as follows: field of view (FOV) =  $15 \times 15 \times 9.6$  cm<sup>3</sup>, acquisition matrix =  $256 \times 256 \times 32$ , TE = 32  $\mu$ s, flip angle =  $5^\circ$ ,

TR = 20 ms, and scan time = 3 minutes 36 seconds. Six healthy volunteers (22–35 years old) were recruited for tibia imaging; the sequence parameters of 3D UTE-Cones were as follows: FOV =  $12 \times 12 \times 16$  cm<sup>3</sup>, matrix =  $192 \times 192 \times 32$ , TE = 32  $\mu$ s, flip angle =  $5^\circ$ , TR = 20 ms, and scan time = 2 minutes 45 seconds. Five healthy volunteers (28–84 years old) were recruited for ankle imaging; the parameters of UTE-Cones imaging were as follows: FOV =  $11 \times 11 \times 6$  cm<sup>3</sup>, matrix =  $256 \times 256 \times 30$ , TE = 32  $\mu$ s, flip angle =  $5^\circ$ , TR = 20 ms, and scan time = 3 minutes 22 seconds. Informed consent was obtained from all subjects in accord with the guidelines of the institutional review board.

## 2.4 | Data analysis

To evaluate both the fat suppression and the water attenuation for the proposed soft-hard composite pulse and the conventional FatSat module, a signal suppression ratio (SSR; unit in percentage), defined as the fraction of the subtracted image between non-fat-suppression image and fat-suppression image by the non-fat-suppression image, was used. A higher SSR value corresponded to better fat suppression or a stronger water attenuation induced by the fat-suppression technique used. Both the pixel-wised SSR maps and region of interest (ROI)-based signal mean and standard deviation values within all tissues were used for comparison. All analysis algorithms were written in Matlab 2017b (The MathWorks Inc., Natick, MA).

## 3 | RESULTS

Numerical simulation results of the excitation profiles or spectrums for the single hard pulse, proposed soft-hard composite pulse, and conventional FatSat module are shown in Figure 2. As can be seen from the transverse magnetization (i.e.,  $M_{xy}$ ) profiles in Figure 2A–F, both the soft-hard and the FatSat pulses were able to null the fat signals at  $-440$  Hz. However, the signal-nulling bandwidth of the soft-hard pulse was narrower than the FatSat pulse, and 2 side lobes appeared in both sides of the fat peak. This was induced by the off-resonance excitation during the soft pulse, when the spin had a different on-resonance frequency than the fat center frequency. However, when tissue  $T_2$  was getting shorter, the profiles approached those of the standard single hard pulses. On the other hand, though there were larger side lobes in the excitation of fatty tissues, they had little effect on the water peak, because of the narrower water spectrum. Consequently, the proposed soft-hard composite pulse had very little effect on both short and long  $T_2$  water signals and therefore generated similar water excitations as the single hard pulse. The FatSat module had a better fat suppression than the soft-hard composite pulse, especially

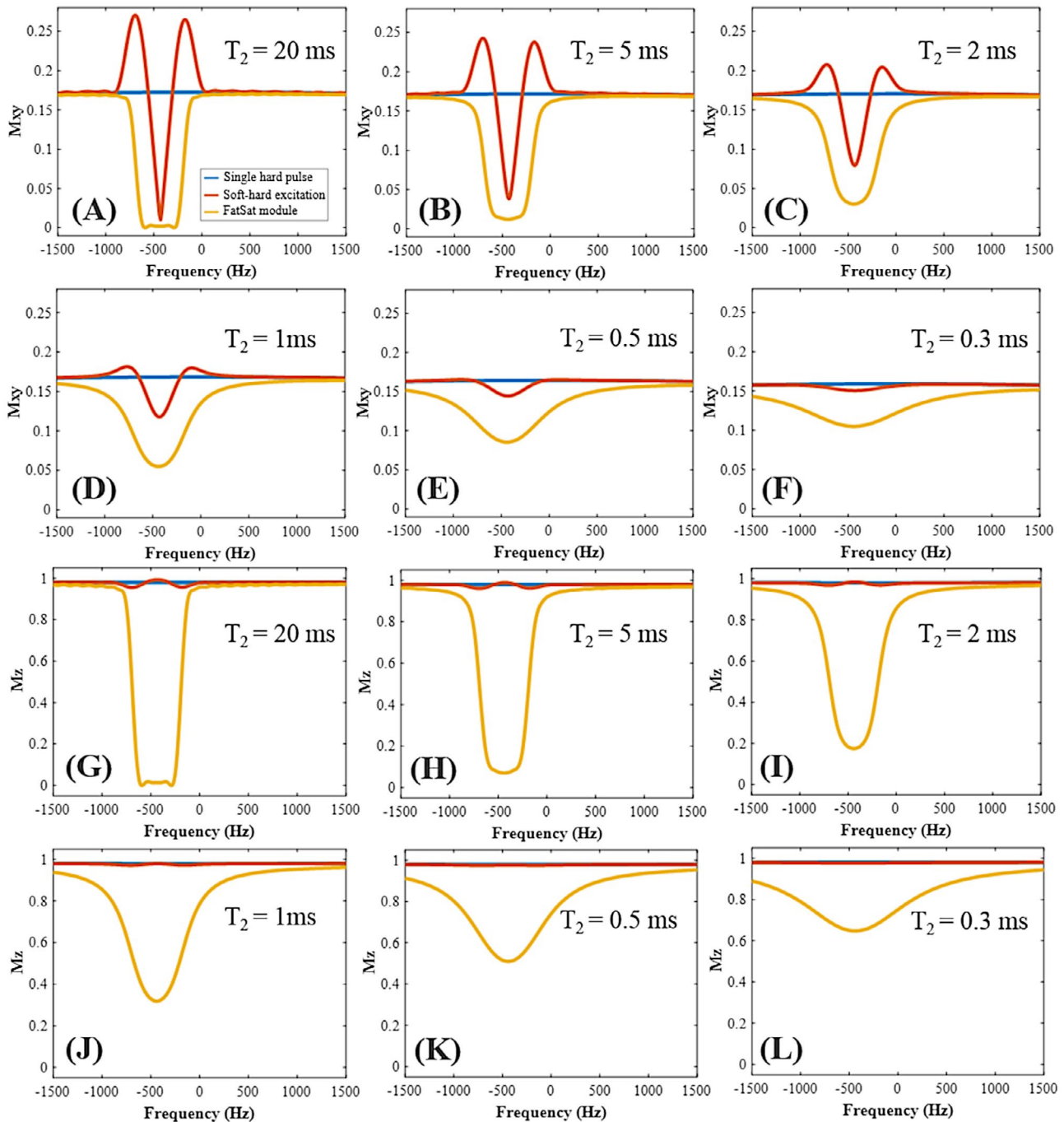


**FIGURE 2** Bloch simulations for the excitations of a single hard pulse (blue curves), the proposed soft-hard composite pulse (red curves), and the conventional FatSat module (yellow curves). Both transverse (A-F) and longitudinal (G-L) magnetization profiles were calculated for tissues with different  $T_2$ s of 20, 5, 2, 1, 0.5, and 0.3 ms. Much lower saturation effect was observed for the proposed soft-hard composite pulse compared with that of the FatSat module

for the tissue with a broad fat spectrum. In comparison, the high flip angle saturation pulse used in the FatSat module led to a strong direct saturation on the broad spectrum short  $T_2$  water signals. Thus, fewer short  $T_2$  signals were excited compared with those generated by the single hard pulse or the soft-hard pulse.

As can be seen from Figure 2G-L, the longitudinal magnetization (i.e.,  $M_z$ ) profiles generated by the soft-hard pulse

is very close to the single hard pulse, which confirms that the soft pulse has little effect on water signals. In contrast, the reduced  $M_z$  profiles of the FatSat module, compared with those in both excitations of the single hard pulse and the soft-hard pulse, demonstrate the strong direct attenuations of the short  $T_2$  signals by the FatSat module.

Simulated UTE imaging results are shown in Figure 3. As evidenced by the  $M_{xy}$  signal curves, higher flip angles



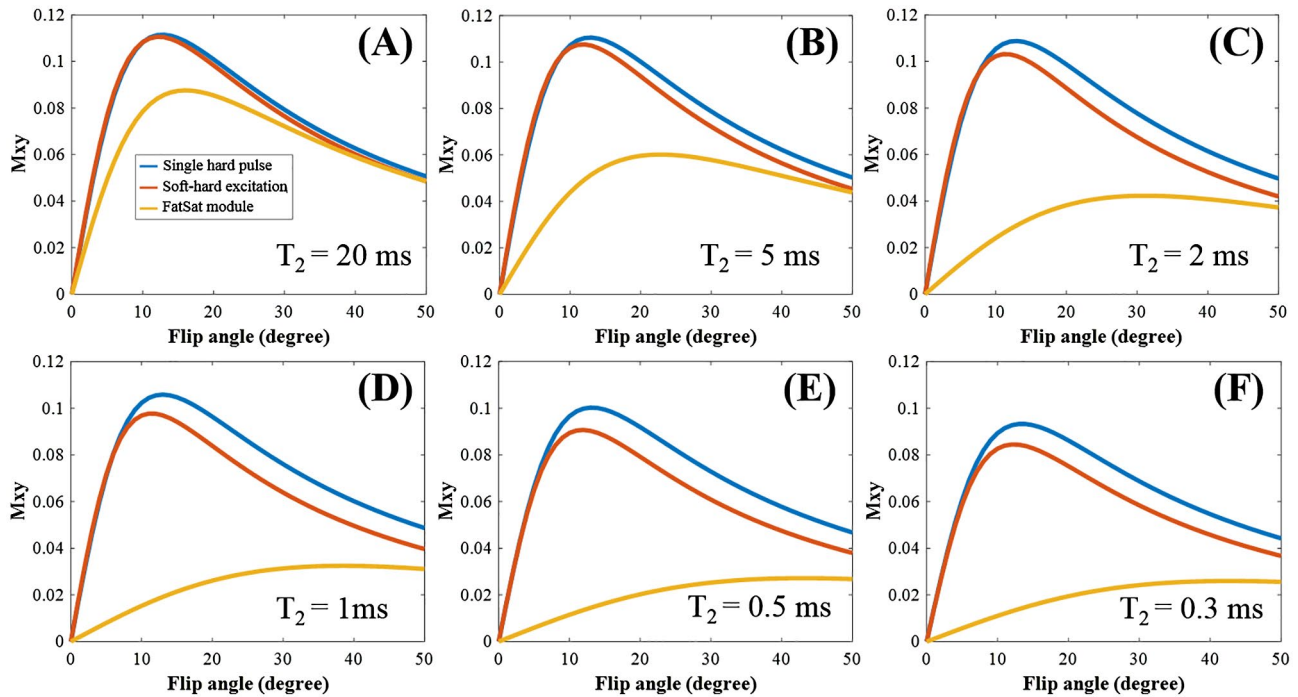


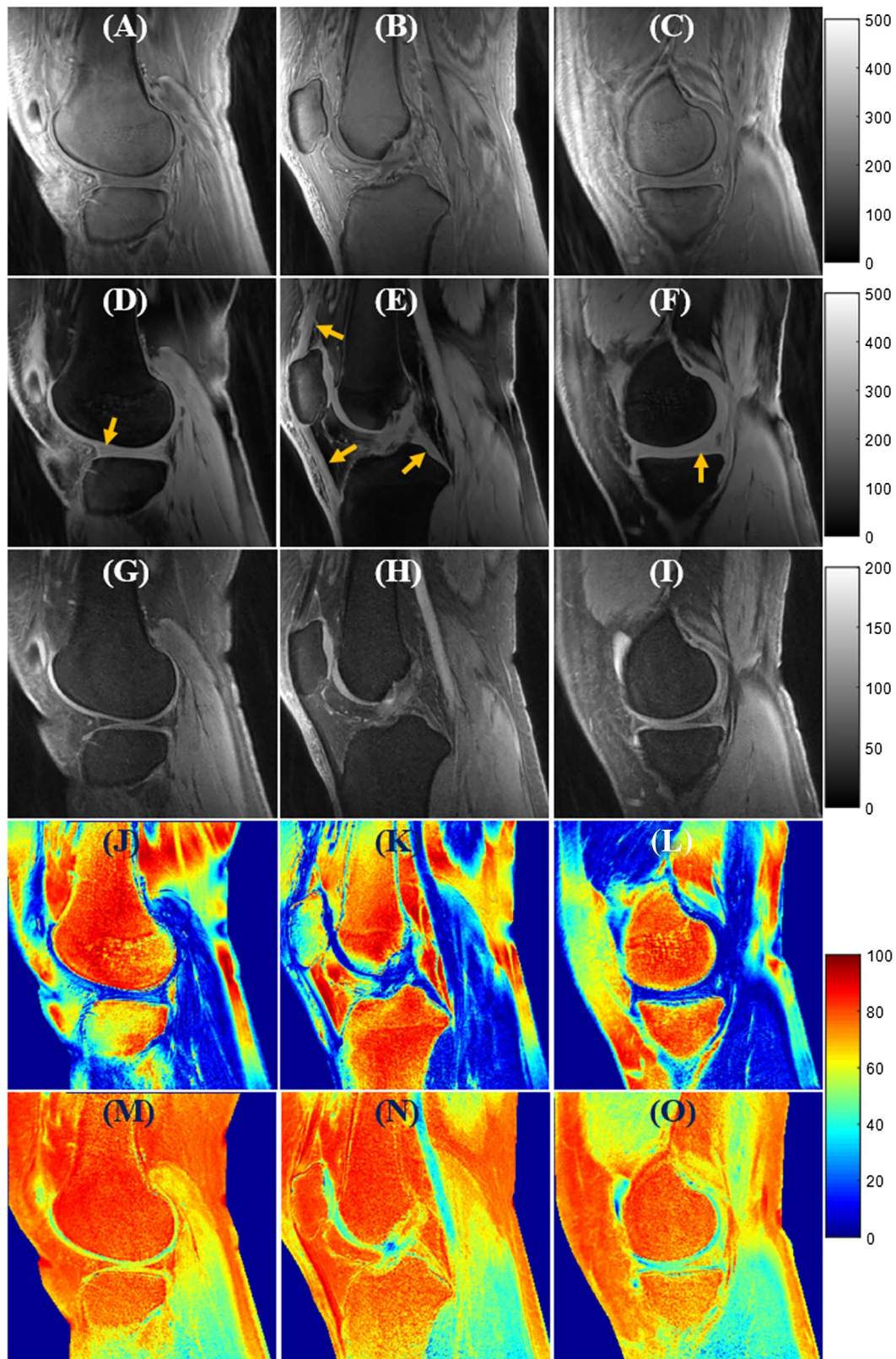
**FIGURE 3** Simulations of UTE imaging using the excitations with a single hard pulse (blue curves), the proposed soft-hard composite pulse (red curves), and the conventional FatSat module (yellow curves), respectively. The UTE signal intensities changed with the flip angles ranged from  $0^\circ$  to  $50^\circ$ . Six different  $T_2$ s of 20, 5, 2, 1, 0.5, and 0.3 ms were used to simulate both long and short  $T_2$  tissues. All the tissue  $T_1$ s were set to a constant value of 800 ms for simulation

demonstrate less-effective excitations compared with the single hard pulse excitation. Stronger signal attenuation is induced by the soft pulse with a higher flip angle. When the excitation flip angles are  $<10^\circ$ , the proposed soft-hard pulse can get similar signal intensities as the single hard pulse for both short and long  $T_2$  tissues. In comparison, the derived signal curves of the FatSat module are much lower than those of the single hard pulse and soft-hard pulse because of the large direct saturations.

Figure 4 shows the in vivo knee UTE-Cones imaging results from a 24-year-old volunteer. The first 3 rows are the grayscale images acquired with the single hard pulse, the proposed soft-hard water excitation pulse, and the conventional FatSat module, respectively. The last 2 rows show the SSR colormaps for the 2 fat suppression methods, respectively. The UTE-Cones images with the excitations of the proposed soft-hard pulse and the product FatSat module both demonstrate good fat suppression and much better image contrast than the non-fat-suppression images. The UTE-Cones images with the excitations of a single hard pulse and the soft-hard pulse are displayed with the same value range (i.e., [0, 500]) because of their similar signal intensity levels. In contrast, the FatSat UTE-Cones images are displayed with a much narrower value range (i.e., [0, 200]) because of their lower maximum signal intensities, which were induced by the strong water attenuations (including both direct saturation and MT effect) of the FatSat module. The short  $T_2$  tissues, such as menisci, patellar

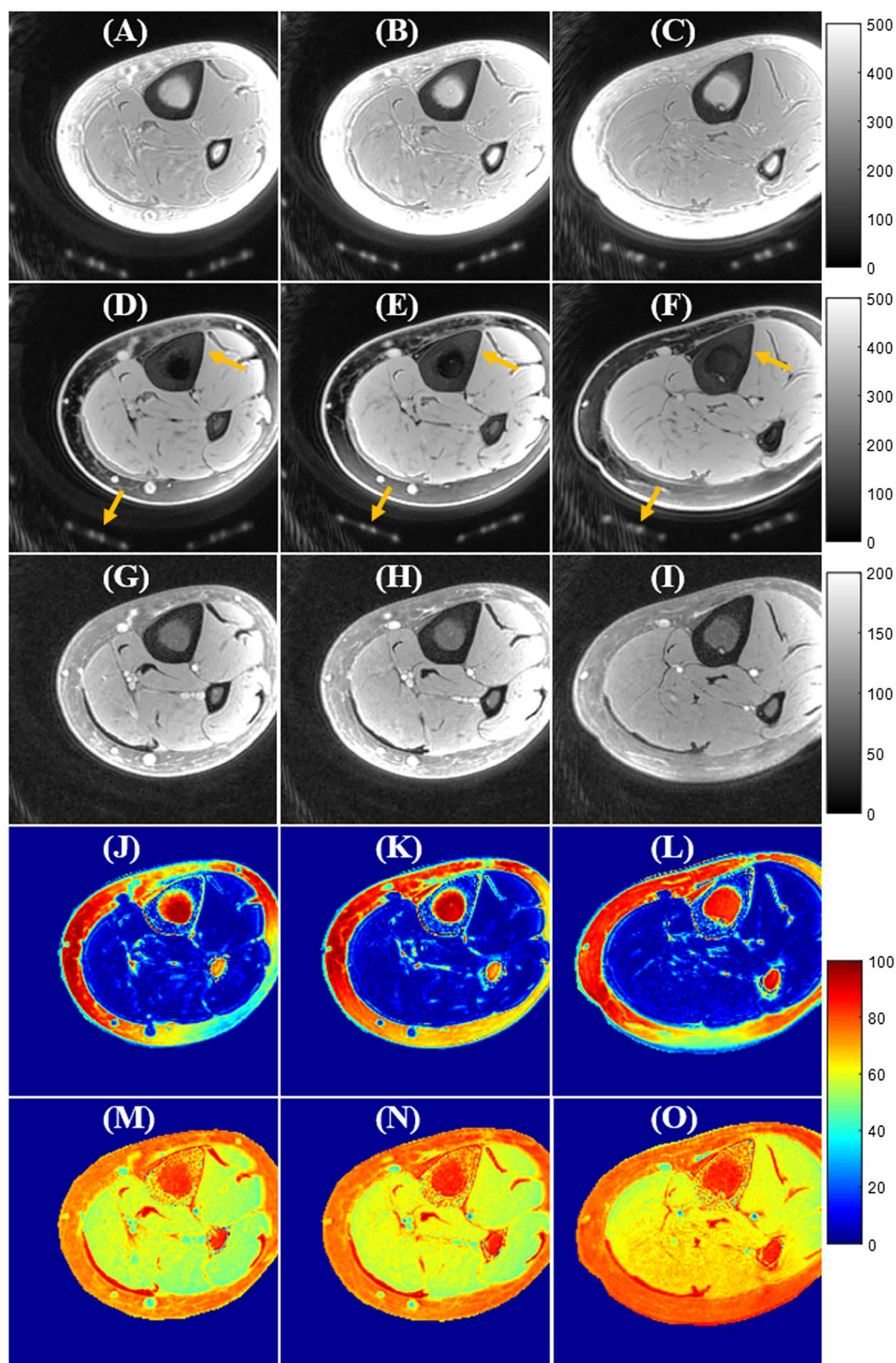
tendon, and posterior cruciate ligament (PCL; indicated by arrows), in the UTE-Cones images with the soft-hard pulse excitation show much better preserved signal intensities than those in the FatSat UTE-Cones images. The SSR maps also suggest that there were nearly no signal attenuations for either short or long  $T_2$  tissues when using the proposed soft-hard pulse for excitation. In comparison, there were strong attenuations for the water signals in the FatSat UTE-Cones images, especially for the short  $T_2$  tissues. Similar to the simulation results, the fat-suppression technique using the soft-hard pulse was less effective and more spatially inhomogeneous than the FatSat module. This is attributed to the narrow nulling bandwidth and the additional side lobes of the soft-hard pulse, which induce increased sensitivity to the  $B_0$  inhomogeneity.

Figure 5 shows in vivo tibial UTE-Cones imaging results from a 35-year-old volunteer. Like the above knee imaging, the UTE-Cones images with the proposed soft-hard composite pulse excitation show excellent image contrast and well-preserved cortical bone and muscle signals. In comparison, most of the short  $T_2$  signals (i.e., cortical bone and coil elements) are lost in the FatSat UTE-Cones images because of the strong saturation effect of the FatSat module. Ex vivo ankle UTE-Cones imaging results from 3 donors are also shown in Supporting Information Figure S1. Much better SNR and higher contrast of short  $T_2$  tendon signals can be seen in the UTE-Cones images with the soft-hard excitation in comparison to the FatSat UTE-Cones images.



**FIGURE 4** In vivo knee joint UTE-Cones imaging (from a 24-year-old volunteer) using excitations with a single hard pulse (A-C), the proposed soft-hard water excitation pulse (D-F), and the conventional FatSat module (G-I). Fat was well suppressed by both the proposed soft-hard pulse and the FatSat module. The short  $T_2$  signals (indicated by yellow arrows in D-F) were much better preserved in the soft-hard excitation images (D-F) compared with FatSat images (G-I). The SSR color maps (soft-hard pulse: J-L; FatSat module: M-O) also suggest that there were almost no signal attenuations for either short or long  $T_2$  tissues when using the proposed soft-hard pulse for excitation. In comparison, there were strong signal attenuations for the water signals in the FatSat UTE-Cones images, especially for the short  $T_2$  tissues





**FIGURE 5** In vivo tibia UTE-Cones imaging (from a 35-year-old volunteer) using excitations with a single hard pulse (A-C), the proposed soft-hard water excitation pulse (D-F), and the conventional FatSat module (G-I). Fat was well suppressed by both the proposed soft-hard pulse and the FatSat module. The cortical bone and coil elements (indicated by yellow arrows in D-F) were much better preserved in the soft-hard excitation images (D-F) compared with FatSat images (G-I). The SSR color maps (soft-hard pulse: J-L; FatSat module: M-O) also suggest that there were almost no signal attenuations for either short or long  $T_2$  tissues when using the proposed soft-hard pulse for excitation. In comparison, there were strong signal attenuations for the water signals in the FatSat UTE-Cones images, especially for the short  $T_2$  tissues



Supporting Information Table S1 summarizes the SSR values for all tissues studied in this work. Both short and long  $T_2$  tissues show much decreased SSRs for the proposed soft-hard pulse compared with those of the FatSat module, demonstrating the proposed excitation pulse's higher excitation efficiency. A slightly lower SSR value was observed for marrow fat with the proposed soft-hard pulse. This is because of the narrower signal-nulling bandwidth of the proposed pulse compared with the conventional FatSat module. The results also show relatively high SSR values for the patellar tendon and anterior cruciate ligament (ACL) with the soft-hard pulse, which may be caused by partial volume and fat contamination in the ROIs of patellar tendon and ACL.

## 4 | DISCUSSION

We have demonstrated in this study that the proposed soft-hard composite pulse is potentially useful for fat suppression in UTE imaging of short  $T_2$  tissues. Numerical simulations show that the proposed soft-hard composite pulse has much lower signal attenuation on water imaging than the conventional FatSat module. In vivo knee and tibia as well as ex vivo ankle UTE imaging demonstrated well-performed fat suppression for the soft-hard pulse excitation. Besides, both the short and long  $T_2$  tissue signals were much better preserved with the soft-hard composite pulse excitation than with the FatSat module for fat suppression. Significantly higher SSRs were achieved with the composite pulse, especially for short  $T_2$  tissues. Such efficient fat-signal suppression may improve MRI-based bone assessments<sup>25-27</sup> and reduce the need for extensive scans for sophisticated multicomponent signal analysis.<sup>28</sup>

The proposed soft-hard composite pulse can preserve the short  $T_2$  signals while suppressing the fat components, thus providing much higher contrast for short  $T_2$  tissues than the non-fat-suppressed images. The soft-hard pulse is relatively sensitive to the  $B_0$  field inhomogeneity because of the narrow bandwidth of the soft pulse. There are also substantial side lobes in the soft-hard pulse excitation that may cause the fat signal to increase in some situations (e.g., in the case where the side lobe locates at the fat peak because of the  $B_0$  inhomogeneity). We can find slightly increased fat signals in some regions with strong  $B_0$  inhomogeneities (e.g., the air-tissue boundary in the middle right of Figure 4D). This phenomenon may occur when the  $B_0$  shift is larger than half of the fat frequency offset (i.e., 1.7 ppm). In our experience with knee imaging, the  $B_0$  inhomogeneity tends to be  $<0.5$  ppm at 3T. To maintain high performance in fat suppression with the soft-hard composite pulse excitation, it is critical to have a system with a relatively uniform  $B_0$  field and/or a high-performing shimming module (e.g., high-order shimming). Though fat

suppression using the soft-hard pulse excitation is less uniform than the conventional FatSat module in this study, the image contrast between water and fat tissues with the soft-hard pulse excitation is still better than the FatSat images according to the calculated SSR values. The soft and hard pulses are 2 independent pulses in our soft-hard composite pulse implementation; thus, the center frequency of the soft pulse can be adjusted to account for  $B_0$  inhomogeneity, if necessary. The proposed soft-hard pulse may be less sensitive to the  $B_1$  inhomogeneity for fat suppression given that the fat components always experience the same flip angles in opposite directions. The minimum phase pulse design can shorten the echo time, thus decreasing the  $T_2$  decay during the soft pulse excitation. Then, the fat magnetization tipped down by the soft pulse can be largely tipped back by the hard pulse, thus allowing more efficient fat suppression.

Two groups have reported that the conventional binomial water excitation pulse provides excellent fat suppression with moderate short  $T_2$  signal attenuations in UTE knee imaging.<sup>29,30</sup> Similar simulations were performed in Springer's study (i.e., Figure 4A) as in our study (i.e., Figure 3).<sup>29</sup> Their simulation results demonstrated a stronger water attenuation with the binomial water excitation pulse when the tissue  $T_2$ s were getting shorter. However, our simulation results of the proposed soft-hard pulse excitation show a better performance in short  $T_2$  tissue imaging, especially when the excitation flip angles are  $<10^\circ$ . Our future studies are expected to compare the above 3 fat suppression techniques for quantitative UTE imaging, such as quantitative measures of  $T_1$ ,<sup>31,32</sup>  $T_{1\rho}$ ,<sup>33,34</sup> bicomponent  $T_2^*$  analysis,<sup>35,36</sup> MT ratio,<sup>37</sup> as well as MT modeling,<sup>38</sup> which will provide more comprehensive understanding about the effect of different fat-suppression schemes.

This study has several limitations. First, we have only demonstrated the technical feasibility of the proposed soft-hard composite pulse for fat suppression and water excitation in UTE imaging of both short and long  $T_2$  tissues. No patients were studied in this work. Second, the proposed soft-hard pulse can only be used for nonselective 3D UTE imaging. A half-sinc pulse together with variable rate selective excitation may be used to replace the short rectangular pulse for slice/slab selective UTE imaging.<sup>39</sup> Third, the effect of the soft-hard composite pulse on quantitative UTE imaging remains to be investigated.

## 5 | CONCLUSION

The proposed soft-hard composite pulse is able to suppress fat signals while preserving both short and long  $T_2$  signals, which is promising for both morphological and quantitative UTE imaging of short  $T_2$  tissues.

## ORCID

Ya-Jun Ma  <https://orcid.org/0000-0003-0830-9232>

Hyungseok Jang  <https://orcid.org/0000-0002-3597-9525>

## REFERENCES

- Robson MD, Gatehouse PD, Bydder M, Bydder GM. Magnetic resonance: an introduction to ultrashort TE (UTE) imaging. *J Comput Assist Tomogr*. 2003;27:825–846.
- Du J, Carl M, Bae WC, et al. Dual inversion recovery ultrashort echo time (DIR-UTE) imaging and quantification of the zone of calcified cartilage (ZCC). *Osteoarthritis Cartilage*. 2013;21:77–85.
- Chang EY, Du J, Bae WC, Chung CB. Qualitative and quantitative ultrashort echo time imaging of musculoskeletal tissues. *Semin Musculoskelet Radiol*. 2015;19:375–386.
- Du J, Carl M, Bydder M, Takahashi A, Chung CB, Bydder GM. Qualitative and quantitative ultrashort echo time (UTE) imaging of cortical bone. *J Magn Reson*. 2010;207:304–311.
- Chen B, Cheng X, Dorth E, et al. Evaluation of normal cadaveric Achilles tendon and enthesis with ultrashort echo time (UTE) magnetic resonance imaging and indentation testing. *NMR Biomed*. 2018;20:e4034.
- Wilhelm MJ, Ong HH, Wehrli SL, et al. Direct magnetic resonance detection of myelin and prospects for quantitative imaging of myelin density. *Proc Natl Acad Sci U S A*. 2012;109:9605–9610.
- Sheth V, Shao H, Chen J, et al. Magnetic resonance imaging of myelin using ultrashort Echo time (UTE) pulse sequences: phantom, specimen, volunteer and multiple sclerosis patient studies. *NeuroImage*. 2016;136:37–44.
- Gatehouse PD, Bydder GM. Magnetic resonance imaging of short T2 components in tissue. *Clin Radiol*. 2003;58:1–19.
- Hennig J, Speck O. *High-Field MR Imaging*. New York, NY: Springer; 2011.
- Del Grande F, Santini F, Herzka DA, et al. Fat-suppression techniques for 3-T MR imaging of the musculoskeletal system. *Radiographics*. 2014;34:217–233.
- Carl M, Nazaran A, Bydder GM, Du J. Effects of fat saturation on short T2 quantification. *Magn Reson Imaging*. 2017;43:6–9.
- Henkelman RM, Stanisz GJ, Graham SJ. Magnetization transfer in MRI: a review. *NMR Biomed*. 2001;14:57–64.
- Pauly JM, Conolly SM, Macovski A. Suppression of long T2 components for short T2 imaging. In *Proceedings of the 10th Annual Meeting of SMRI*, New York, NY, 1992. p. 330.
- Larson PE, Gurney PT, Nayak K, Gold GE, Pauly JM, Nishimura DG. Designing long-T2 suppression pulses for ultrashort echo time imaging. *Magn Reson Med*. 2006;56:94–103.
- Larson PE, Conolly SM, Pauly JM, Nishimura DG. Using adiabatic inversion pulses for long-T2 suppression in ultrashort echo time (UTE) imaging. *Magn Reson Med*. 2007;58:952–961.
- Du J, Takahashi AM, Bae WC, Chung CB, Bydder GM. Dual inversion recovery, ultrashort echo time (DIR UTE) imaging: creating high contrast for short-T2 species. *Magn Reson Med*. 2010;63:447–455.
- Carl M, Bydder GM, Du J. UTE imaging with simultaneous water and fat signal suppression using a time-efficient multispoke inversion recovery pulse sequence. *Magn Reson Med*. 2016;76:577–582.
- Ma YJ, Zhu Y, Lu X, Carl M, Chang EY, Du J. Short T2 imaging using a 3D double adiabatic inversion recovery prepared ultrashort echo time cones (3D DIR-UTE-Cones) sequence. *Magn Reson Med*. 2018;79:2555–2563.
- Li S, Ma L, Chang EY, et al. Effects of inversion time on inversion recovery prepared ultrashort echo time (IR-UTE) imaging of bound and pore water in cortical bone. *NMR Biomed*. 2015;28:70–78.
- Fan SJ, Ma Y, Zhu Y, et al. Yet more evidence that myelin protons can be directly imaged with Ute sequences on a clinical 3 T scanner: Bicomponent analysis of native and deuterated ovine brain specimens. *Magn Reson Med*. 2018;80:538–547.
- Jang H, Carl M, Ma Y, et al. Fat suppression for ultrashort echo time imaging using a single-point Dixon method. *NMR Biomed*. 2019;15:e4069.
- Wang K, Yu H, Brittain JH, Reeder SB, Du J. k-space water-fat decomposition with T2\* estimation and multifrequency fat spectrum modeling for ultrashort echo time imaging. *J Magn Reson Imaging*. 2010;1(31):1027–1034.
- Du J, Hamilton G, Takahashi A, Bydder M, Chung CB. Ultrashort echo time spectroscopic imaging (UTESI) of cortical bone. *Magn Reson Med*. 2007;58:1001–1009.
- Pauly JM, Le Roux P, Nishimura DG, Macovski A. Parameter relations for the Shinnar-Le Roux selective excitation pulse design algorithm. *IEEE Trans Med Imaging*. 1991;10:53–65.
- Jerban S, Ma Y, Nazaran A, et al. Detecting stress injury (fatigue fracture) in fibular cortical bone using quantitative ultrashort echo time-magnetization transfer (UTE-MT): an ex vivo study. *NMR Biomed*. 2018;31:e3994.
- Jerban S, Ma Y, Wong JH, et al. Ultrashort echo time magnetic resonance imaging (UTE-MRI) of cortical bone correlates well with histomorphometric assessment of bone microstructure. *Bone*. 2019;123:8–17.
- Jerban S, Ma Y, Wan L, et al. Collagen proton fraction from ultrashort echo time magnetization transfer (UTE-MT) MRI modelling correlates significantly with cortical bone porosity measured with micro-computed tomography ( $\mu$ CT). *NMR Biomed*. 2019;32:1–10.
- Lu X, Jerban S, Wan L, et al. Three dimensional ultrashort echo time imaging with tri-component analysis for human cortical bone. *Magn Reson Med*. 2019;82:348–355.
- Springer F, Steidle G, Martirosian P, et al. Quick water-selective excitation of fast relaxing tissues with 3D UTE sequences. *Magn Reson Med*. 2014;71:534–543.
- Deligianni X, Bär P, Scheffler K, Trattnig S, Bieri O. Water-selective excitation of short T2 species with binomial pulses. *Magn Reson Med*. 2014;72:800–805.
- Ma YJ, Lu X, Carl M, et al. Accurate T1 mapping of short T2 tissues using a three-dimensional ultrashort echo time cones actual flip angle imaging variable repetition time (3D UTE-Cones AFI-VTR) method. *Magn Reson Med*. 2018;80:598–608.
- Ma YJ, Zhao W, Wan L, et al. Whole knee joint T1 values measured in vivo at 3T by combined 3D ultrashort echo time cones actual flip angle and variable flip angle method. *Magn Reson Med*. 2019;81:1634–1644.
- Du J, Carl M, Diaz E, et al. Ultrashort TE T1rho (UTE-T1rho) imaging of the Achilles tendon and meniscus. *Magn Reson Med*. 2010;64:834–842.
- Ma YJ, Carl M, Searleman A, Lu X, Chang EY, Du J. 3D adiabatic T1p prepared ultrashort echo time cones sequence for whole knee imaging. *Magn Reson Med*. 2018;80:1429–1439.
- Du J, Diaz E, Carl M, Bae W, Chung CB, Bydder GM. Ultrashort echo time imaging with bicomponent analysis. *Magn Reson Med*. 2012;67:645–649.

36. Seifert AC, Wehrli SL, Wehrli FW. Bi-component T2\* analysis of bound and pore bone water fractions fails at high field strengths. *NMR Biomed*. 2015;28:861–872.
37. Grosse U, Syha R, Martirosian P, et al. Ultrashort echo time MR imaging with offresonance saturation for characterization of pathologically altered Achilles tendons at 3 T. *Magn Reson Med*. 2013;70:184–192.
38. Ma YJ, Shao H, Du J, Chang EY. Ultrashort echo time magnetization transfer (UTE-MT) imaging and modeling: magic angle independent biomarkers of tissue properties. *NMR Biomed*. 2016;29:1546–1552.
39. Hargreaves BA, Cunningham CH, Nishimura DG, Conolly SM. Variable-rate selective excitation for rapid MRI sequences. *Magn Reson Med*. 2004;52:590–597.

## SUPPORTING INFORMATION

Additional supporting information may be found online in the Supporting Information section at the end of the article.

**FIGURE S1** In vitro ankle UTE-Cones imaging (28-, 74-, and 84-year-old donors) using excitations with a single hard pulse (A-C), the proposed soft-hard water excitation pulse (D-F), and the conventional FatSat module (G-I). Fat was well

suppressed by both the proposed soft-hard pulse and the FatSat module. The short T<sub>2</sub> tendon signal (indicated by yellow arrows in D-F) was much better preserved in the soft-hard excitation images (D-F) compared with FatSat images (G-I). The SSR color maps (soft-hard pulse: J-L; FatSat module: M-O) also suggest that there were almost no signal attenuations for either short or long T<sub>2</sub> tissues when using the proposed soft-hard pulse for excitation. In comparison, there were strong signal attenuations for the water signals in the FatSat UTE-Cones images, especially for the short T<sub>2</sub> tissues

**TABLE S1** Mean and standard deviations of SSR values (%) of marrow fat, menisci, cartilage, quadriceps tendon, patellar tendon, ACL, PCL, cortical bone, Achilles tendon, and muscle in the knee, tibia, and ankle studies

**How to cite this article:** Ma Y-J, Jerban S, Jang H, Chang EY, Du J. Fat suppression for ultrashort echo time imaging using a novel soft-hard composite radiofrequency pulse. *Magn Reson Med*. 2019;82: 2178–2187. <https://doi.org/10.1002/mrm.27885>